Original Article

http://dx.doi.org/10.4322/2176-1523.1332

STUDY OF FLOW MODIFICATION AND INCLUSION REMOVAL IN SLAB TUNDISH DUE TO BOTTOM GAS INJECTION

Heric Henrique Souza e Silva [1]
Carlos Antônio da Silva [2]
Itavahn Alves da Silva [2]
Antônio Gurgel Barros Júnior [2]

Abstract

In order to quantify inclusion removal the role of flow pattern inside the tundish is assessed. Also mathematical models of inclusion separation including the influence of inclusion coalescence are discussed. This analysis suggest that as far as small size inclusions are concerned, operational parameters such as piston flow fraction are not important since for them the probability of separation is negligible. However, techniques such as gas curtains are to be considered for better inclusion control. Mathematical and physical modeling results are presented considering association of a porous dam and a ring shaped injection plug positioned around the strand. The results confirm the theoretical expectations as the flow modification, revealed by the mathematical simulation, allows the imprisonment of particles in the reactor and so the fraction of small inclusions leaving the tundish stays under 3% for the gas-assisted strand.
Keywords: Tundish; Inclusion removal; Fluid flow; Gas curtain.

ESTUDO DE MODIFICAÇÃO DE FLUXO E REMOÇÃO DE INCLUSÕES EM UM DISTRIBUIDOR DE LINGOTAMENTO DE PLACAS DEVIDO A INJEÇÃO DE GÁS PELO FUNDO

Resumo

Com o intuito de quantificar o papel da remoção de inclusões, avalia-se o padrão de fluxo no interior do distribuidor. Modelos matemáticos de separação de inclusão, incluindo a influência da coalescência de inclusões também são discutidos. A presente análise sugere que no tocante a inclusões de pequenas dimensões, parâmetros operacionais como fração de fluxo pistonado deixam de ser críticos, uma vez que a probabilidade de separação é desprezível. Entretanto, técnicas como o uso de cortina de gás são relevantes para melhor controle do conteúdo de inclusão. Resultados de modelamento físico e matemático são apresentados considerando a associação de uma barreira porosa e um plugue anelar de injeção posicionado ao redor do veio. Os resultados confirmam as expectativas já que a modificação de fluxo, exposta pela simulação matemática, permite que inclusões fiquem retidas no reator, registrando valores de saída abaixo de 3% no caso do veio com aspersão de gás.
Palavras-chave: Distribuidor; Remoção de inclusão; Fluxo de fluido; Cortina de gás.

1 INTRODUCTION

The tundish in steel concast machines has become an important metallurgical reactor, acquiring an essential role for steel cleanness and surpassing the original function as a buffer between the batch secondary metallurgy of ladles and the continuous casting. As the last opportunity to act in the molten flow before the solidification, interventions are usually made in order to maximize residence time, reduce the amount of solid inclusions leaving at the strands, assure chemical and temperature homogenization and adjust the desired steel grade. Inclusion removal in a continuous casting tundish is usually linked to the liquid flow pattern. Flow pattern is commonly characterized through a combined

[1] *Rede Temática em Engenharia de Materiais – REDEMAT, Universidade Federal de Ouro Preto – UFOP, Ouro Preto, MG, Brasil. E-mail: herichsilva@yahoo.com.br*
[2] *Departamento de Engenharia Metalúrgica e de Materiais, Universidade Federal de Ouro Preto – UFOP, Ouro Preto, MG, Brasil.*

flow model yielding fraction of piston flow, fraction of perfect mixing and fraction of dead volume [1]. Customarily, larger fractions of piston flow are associated with a better inclusion removal; dead volumes are linked to lower efficiency of volume utilization. Tripathi et al. [2] suggested an improvement of the tundish operation by deploying a well-shaped bottom while Merder [3] stated the variations that can outcome from different impact pads geometry. Combining both scenarios Cwudzinski [4] displayed the flow pattern using physical and computational modeling. There are a few references in the literature regarding the use of gas injection into the tundish, as an auxiliary tool for inclusion removal. Inclusion removal would increase due to: modification of the flow pattern, with the redirection of flow toward the slag layer; activation of the collision – coalescence – flotation mechanism; direct flotation of inclusions due to its attachment to the rising bubbles. Rogler [5], Seshadri et al. [6] have examined some theoretical aspects of gas – particle interaction in a tundish. Accordingly, the chance of a gas – particle collision and attachment followed by removal from the tundish increases with increasing length of porous injection device and gas flow rate and with decreasing gas bubble size. However, the outcome is also dependent on injection element shape and location relative to the strand outlet; this work deals with results regarding a special injection device.

2 METHODOLOGY

A macroscopic analysis of the influence of the overall features of the flow field on inclusion removal is performed. This analysis suggests that inclusions of smaller sizes will be hardly removed in the tundish; also inclusion collision-coalescence-flotation phenomenon will be not significant. Then, the performance of a particular arrangement of gas curtain devices is analyzed using mathematical and physical simulations.

2.1 Influence of Overall Features of Flow Field on Inclusion Removal

The most simple flow configuration is one of a perfect mixing region (nearby the steel entrance) followed by a piston flow region. This scenario can be further complicated by the existence of a dead volume region and/or a short-circuiting, Figure 1.

In order to assess the likelihood of inclusion removal typical steelmaking data as shown in Table 1 are taken in consideration. Inclusion concentration at tundish entrance, at an imaginary boundary between perfect mixing and piston flow region, and at tundish exit can symbolized by C_o (-/m^3), C_1 (-/m^3) e C_2 (-/m^3), respectively. It has been proposed that [7].

$$\frac{C_1}{C_o} = e^{-\frac{Vasc.\ \alpha\ L}{Vsteel\ .\ Ho}} \quad (1)$$

Preliminary calculation using data from Table 1 show that the exponent of Equation 1 is small enough to allow a simplification, as shown in Equation 2 (following Taylor's series):

$$\frac{Co - Cl}{Co} = \frac{Vasc\ .\ \alpha L}{Vsteel\ .\ Ho} \quad (2)$$

Usually one assumes a velocity profile such as all velocity vectors are horizontal and of same intensity inside the piston flow region. Also is taken that the inclusion motion is a combination of a horizontal motion with a velocity equal to V_{steel} and a vertical motion with velocity equal to V_{asc}. Equations 3 and 4 result from these considerations.

$$\frac{C_2}{C_1} = 1 - \frac{V_{asc}\dfrac{(1-\alpha)\ L}{Vsteel}}{Ho} = 1\ \frac{V_{asc}(1-\alpha)L}{Vsteel\ .\ Ho} \quad (3)$$

$$\frac{C_1 - C_2}{C_1} = \frac{V_{asc}(1-\alpha)L}{Vsteel\ .\ Ho} = \frac{V_{asc}(1-\alpha)L}{Q/W} \quad (4)$$

Equation 1 and typical data from Table 1 suggest that 99.96% of the 30 μm inclusions still remain in steel after the perfect mixing region; by the same token, see Equation 3, 99.38% of the 30 μm inclusions remains in the steel after going through the piston flow region; thus the overall fraction of inclusions drawn to the mold would be 98,97%. Then the likelihood of small size inclusion removal is dim. The odds will increase for larger sizes since the ascension

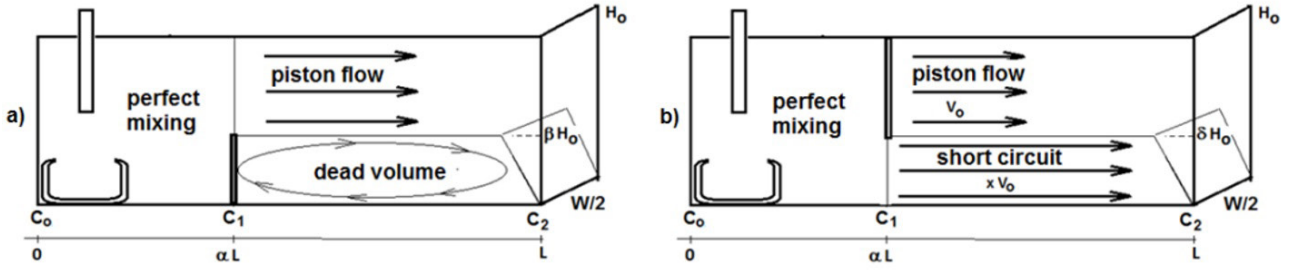

Figure 1. Schematics of longitudinal tundish cross section depicting fractions of perfect mixing and piston flow for two scenarios a) with dead volume b) with short circuit.

velocity roughly increases with the square of the diameter. However exactly the small size inclusion poses the major problem to steel quality. This preliminary evaluation does not take in consideration the existence of dead volume region, of short circuiting and inclusion coalescence within the perfect mixing zone (due to stirring and differential velocity effects). Some of these effects are discussed as follows. As suggested in Figure 1b a turbulence inhibitor acts to confine the agitation/stirring to a region nearby the ceramic valve, defining the perfect mixing regions. Also the steel/inclusion flow can be redirected to the slag/metal interface where inclusions will be attached. However a too strong flow can lead to slag entrainment. Another effect of flow modifier such as turbulence inhibitors could be a dead volume region (a recirculation volume) close to the bottom of the tundish, with a volume proportional to βH_o. The main flow is then restricted to the upper portions of the tundish and it is easy to show that although the inclusion is directed to the upper slag layer the average velocity must increase in order to keep the same volumetric flow rate, leading to smaller residence time. Thus, the fraction of inclusions is given by Equation 5.

$$\frac{C_1 - C_2}{C_1} = \frac{Vasc\ (1-\alpha)L}{\frac{Q}{W(1-\beta)\ Ho}\ \{(1-\beta)Ho\}} = \frac{V_{asc}(1-\alpha)L}{Q/W} \quad (5)$$

Which is the same result as shown in Equation 4; no further improvement should be expected for this flow pattern. Additionally, a faster flow directed to the surface can be detrimental. Allied to interfacial turbulence the result could be slag entrainment, a result opposed to the required. Short circuiting can be modeled assuming that ahead of the perfect mixing region there are two layers of liquid, each moving at a specific velocity. The upper layer moves with velocity V_o, the lower layer with velocity equal to xV_o ($x>1$), but keeping the same steel average velocity, Figure 1b. This calculation can be done based on a reactor combination comprised of a perfect mixing reactor (I) feeding two piston flow reactors, (II) and (III), as shown in Figure 2.

As part of short circuit definition the flow inside reactor III should be faster than the flow inside reactor II. The fraction of inclusion removal can be estimated assuming that inclusions inside the faster flow (lower piston flow, short circuit) report to the strand and that some of the inclusion inside the upper piston flow reactor could reach the slag/metal interface. Taking data from Table 1, assigning arbitrary values of $X = 5$; $\delta = 0.05$, which means $V_o = 0.006944$ m/s, one estimates no remarkable effects on inclusion removal: 99.26% of them reports to the strand.

A model of inclusion coalescence due to differential velocity (Stokes' Law) and stirring has been developed to account for phenomena occurring at the perfect mixing region. It is based on Saffman & Turner model [8]. Accordingly, the size distribution evolves when inclusions of different sizes hit each other and coalesce; break up is not taken in consideration. A population balance accounts for death and birth of inclusions. Thus the number of inclusions to be added to the k_{th} class, per unit volume and time, such as $R_{k-1} \leq R_{aver} \leq R_k$, is given by Equations 6, 7 and 8.

Table 1. Typical continuous casting values relative to tundish operation

Variable	Symbol	Value	Variable	Symbol	Value
Tundish length	L	4.5 m	Steel density	ρ_{steel}	7000 kg/m^3
Tundish width	W	0.8 m	Steel viscosity	η	0.007 Pa.s
Tundish depth	Ho	1.5 m	Inclusion density	ρ_I	3000 kg/m3
Throughput	P	4.2 ton/min	Inclusion diameter	d	30μm
Steel flow rate	Q	0.01 m^3/s	Fraction of piston flow	α	0.4
Inclusion ascension velocity (Stokes' Law)	V_{asc}	2.857x10^{-5} m/s	Average steel velocity	V_{steel}	0.00833 m/s
Steel velocity at nozzle	V_{VL}	3.8 m/s			

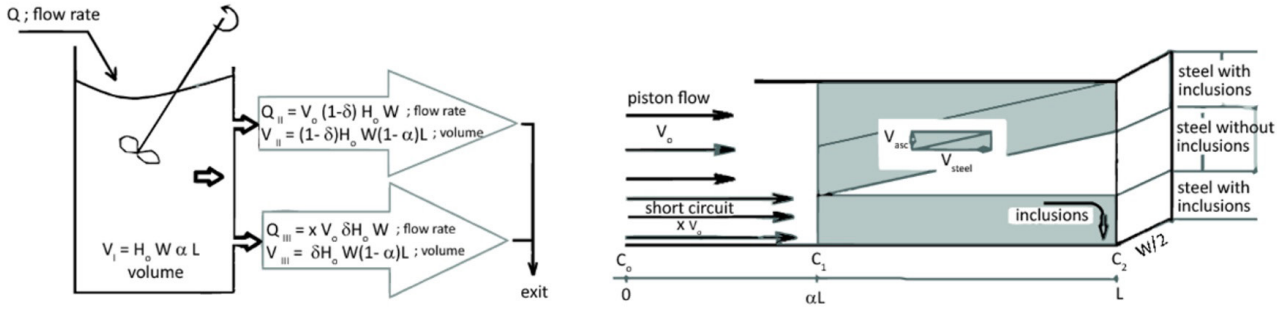

Figure 2. Reactor combination for short circuiting evaluation.

$$\frac{dN}{dt}\left[\frac{inclusions}{m^3 s}\right] = N_i \ . N_{i+n} \ . \sum \beta \tag{6}$$

$$\beta\left(v_i \ , v_j\right) = \pi\left(R_i - R_j\right)^2 . \left|v_i - v_j\right| m^3 / s \tag{7}$$

$$\beta\left(v_i \ , v_j\right) = \alpha_T \ 1.3\left(R_i + R_j\right)^3 . \left(\frac{\varepsilon}{\mu / \rho}\right) m^3 / s \tag{8}$$

where β is a proportionality constant which is a function of the acting mechanism (Stokes' law, stirring) ; R_i and R_j [m] are radii of inclusions of the ith and jth classes; v_i and v_j their flotation velocities [m/s]; ε [m^2/s^3] and μ [m^2/s] are the rate of dissipation of kinetic energy of turbulence and steel kinematic viscosity, respectively. The α_T parameter is known as a coalescence coefficient; the number of inclusions of the k_{th} class increases but restricted to mass conservation, Equation 9.

$$R_{aver} = \{R_i^3 + R_{i+n}^3\}^{1/3} \tag{9}$$

Likewise the birth of new inclusions of k_{th} class assumes the death of inclusions of classes i and i+n. This set of equation allows estimating the size distribution as a function of time given the initial oxygen content and a presumed initial size distribution. Here initial means outcoming the ceramic nozzle, at tundish entrance. Finally it is assumed that each inclusion colliding into metal/slag interface remains attached to it. This collision represents a death contribution to the population balance. Ansys CFX software has been used to estimate the distribution of rate of dissipation of kinetic energy of turbulence inside a tundish. Due to symmetry a quarter of the tundish, Figure 3a, was taken in consideration and the flow conditions (boundary conditions) reflected those in Table 1. A volume right above the turbulence inhibitor was ascribed to the perfect mixing region as it is shown in Figure 3b; although arbitrary this regions depicts the highest levels of turbulence.

As far as boundary conditions are concerned non slipping conditions have been applied to all metal refractory interfaces (velocity equal to zero, rate of dissipation of kinetic energy of turbulence, turbulence kinetic energy equal to zero). A flat velocity profile at the tundish entrance (outlet of the ceramic nozzle) is assumed. As a boundary condition kinetic turbulence energy and rate of dissipation of kinetic energy of turbulence have been assumed as shown in Equations 10 and 11:

$$K = 0.01 * V^2 m^2 / s^2 \tag{10}$$

$$\varepsilon = K^{1.5} / R \ m^2 / s^3 \tag{11}$$

here K is the kinetic energy of turbulence; V is the average velocity inside the ceramic nozzle; ε is the rate of dissipation of kinetic energy of turbulence; R is the radius of the ceramic nozzle.

The volume of the perfect mixing region has been chosen in order to encompass the region of highest levels of kinetic energy of turbulence. As shown in Figure 3b this is the region above the turbulence inhibitor. It can be initially assumed to exist a relationship between the incoming steel jet power input and the rate of dissipation of kinetic energy. The power input can be estimated as in Equation 12.

$$P = \left(\rho.V.A.V\right).V = \rho.A.V^3 = \left(\rho / A^2\right) \times Q^3 \tag{12}$$

here: ρ is the steel density; A is the cross sectional area of the ceramic nozzle; V is the average steel velocity inside the nozzle; Q is the volumetric flow rate.

Simulations results with steel flow rates within the 0.00864 m^3/s to 0.0121 m^3/s range, yields, for this particular tundish, the rate of dissipation of kinetic energy of turbulence can be calculated by Equation13:

$$\varepsilon = 0.0044 * V^3 + 5 * 10^{-5} R^2 = 0.9999 \tag{13}$$

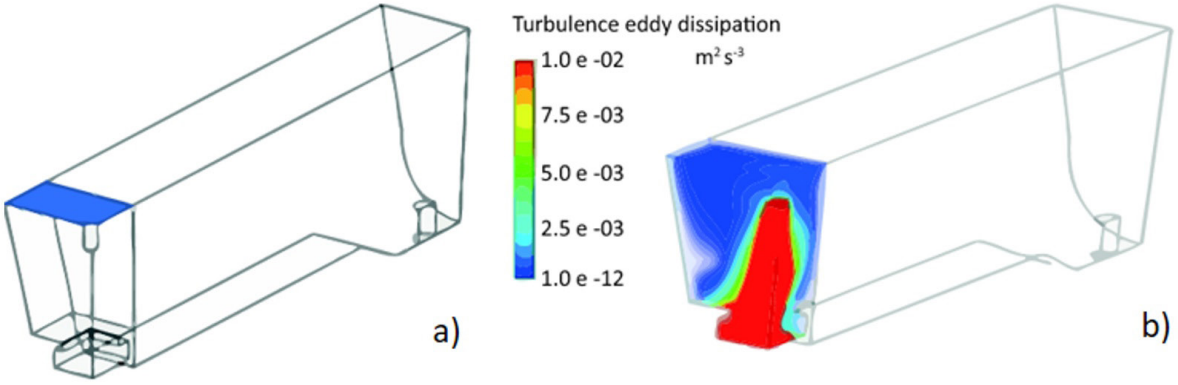

Figure 3. Geometrical configuration of quarter of tundish used for CFD.a) surface above turbulence inhibitor b) volume right above turbulence inhibitor, contour of turbulence edge dissipation.

The initial oxygen concentration was taken as 20 ppm and as a measurement of the inclusion content. The initial size distribution is not known; a normal distribution is then assumed since the goal is to perform comparative studies. As it is expected the steel flow rate influences both the rate of energy dissipation and the average residence time inside the perfect mixing region. These effects are shown in Table 2. The influence of collision and coalescence of inclusions is summarized on Figure 4.

The influence of flow rate is not remarkable. Smaller steel velocities lead to smaller values of rates of dissipation of kinetic energy but also to larger residence times. The effects seem to cancel each other. 15% of the inclusions are removed for higher velocities, 17% of inclusions are removed for smaller velocities. There is a small effect on size distribution as shown in Figure 4b. The size distribution moves itself to larger values as a result of higher agitation (steel velocities). However, this effect does not seem to be sizable. That could be due to a small inclusion population (20 ppm of oxygen) and small residence time. Collision and coalescence could contribute to steel cleanness if turbulence is not excessive; the later could lead to slag entrainment being counterproductive. According to these calculations, the average size of inclusions hauled to the piston flow region would not change in a noticeable way.

2.2 Mathematical and Physical Simulation of a Tundish Operation with a Gas Curtain

A set of experiments has been designed to assess the performance of a given gas injection system. A tundish model built in acrylic and following a scale factor $\lambda = 1{:}4$ was used. The experimental scheme is depicted in Figure 5. Tundish capacity is close to 72 tons and typical throughput is 4.5 ton/min per strand.

The submerged valves were replaced by calibrated valves (metering nozzles), so that the liquid flow rate was held constant for a certain liquid level on the tundish. Standard 63 μ m sieves were placed at each tundish outlet in order to retain the plastic particles used to simulate the inclusions. An emulsion of plastic particles in water – alcohol solution was injected by a peristaltic pump during 50 minutes. The plastic particles collected at each sieve were oven dried and weighted. Gas flow rate, 1 to 3 lpm, was chosen as a compromise between a value high enough to achieve the desired inclusion removal but without excessive metal/slag interface disturbance. A typical inclusion in steel has density of 3000 kg / m^3; the steel is around 7000 kg/m^3. On the other hand water and plastic particles densities and close to each other, 1000 kg/m^3 and 970 kg/m^3. To achieve the same driving force for the separation of inclusions, assumed to be due

Table 2. Rate of dissipation of kinetic energy of turbulence and average residence time inside the perfect mixing region for various steel flow rates

Average velocity inside the ceramic nozzle (m/s)	Flow rate (m^3/s)	Volume of perfect mixing (m^3)	Average residence time (s)	Rate of dissipation of kinetic energy (m^2/s^3)
0.77636	0.008064	0.6624	82.14	0.00206
0.97045	0.01008	0.6624	65.71	0.00402
1.16454	0.012096	0.6624	54.76	0.00698

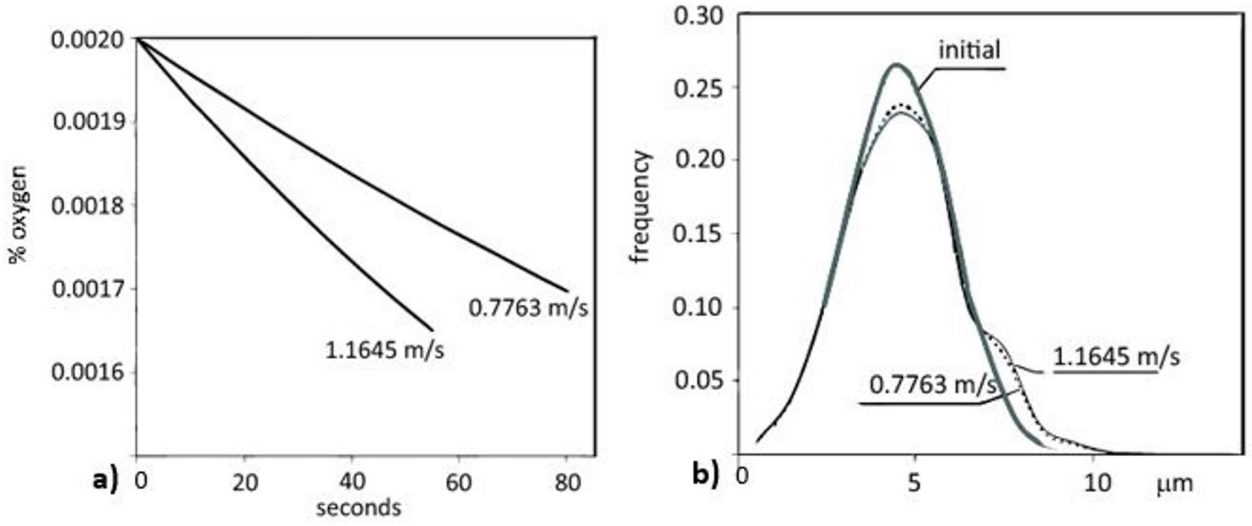

Figure 4. (a) Influence of steel flow rate on oxygen (inclusion content) due to collision – coalescence phenomena inside the perfect mixing region; (b) Inclusion size distribution at the perfect mixing region exit as a function of steel velocity.

to buoyancy, the particles used in the model should larger than the actual inclusions. According to Sahai and Emi [9] a similarity criterion would read, in Equation 14.

$$d_m / d_{ind} = \left\{ (1-\rho_I / \rho_L)_{ind}^{1/2} \Big/ (1-\rho_I / \rho_L)_m^{1/2} \right\} \lambda^{-0.25} \quad (14)$$

Here "m" refers to the model; "ind" refers to industrial conditions. This relationship assumes a model operated according to the Froude similarity criterion, which provides as relationship between volumetric flow rates in Equation 15.

$$Q_m = Q_{Ind} \lambda^{2.5} \quad (15)$$

Following this argument micronized particles of plastic were used in the range of 50 to 100μm and 100-200μm. Two gas injection devices have been tested: a porous ring with internal and external radii of 0.10 m and 0.12 m placed around the strand outlet; a porous dam with a width of 0.01m placed between the strand outlet and turbulence inhibitor; a combination of these two.

Figure 6 shows an isometric view of the tundish. For simulation purposes half a tundish was taken assuming symmetry relative to a vertical plane passing through the center of the strand outlet. A mesh with 2280000 tetrahedral elements was implemented in order to solve Navier Stokes, Continuity and Realizable k-ε model of turbulence equations using Ansys Fluent. Liquid was taken as a continuous phase and gas bubbles as disperse phase in an Eulerian-Eulerian scheme. Bubble sizes were defined according to experimental measurement. The top liquid gas interface was taken as a semi porous membrane allowing gas passage only. The usual non-slipping condition at all solid surface was considered.

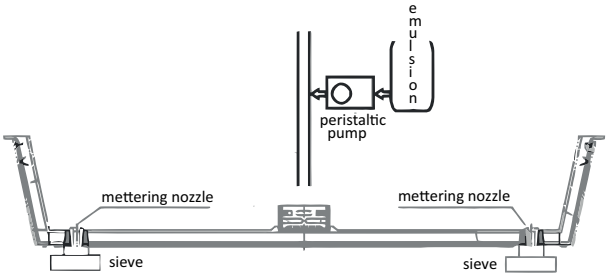

Figure 5. Experimental setup.

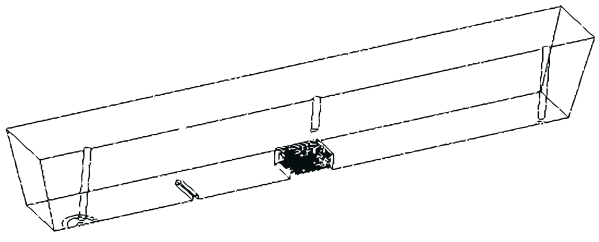

Figure 6. Schematic view of tundish geometry used for mathematical simulation.

3 RESULTS

Gas bubble size distribution was evaluated through a series of photographs taken at the gas curtain under a fixed gas flow rate. The average diameter of bubble and standard deviation are 0.674 and 0.12 respectively as measured from a 100 bubbles population. The inclusion separation efficiency can be measured by the ratio of material collected at a given strand and the total collected at both strands. Equation 16 an 17 estimate these efficiencies:

$$E1 = \begin{pmatrix} mass\ collected \\ at\ strand \\ with\ air\ injection \end{pmatrix} / \left(total\ mass\right) x\ 100 \quad (16)$$

$$E2 = \begin{pmatrix} mass\ collected\ at \\ strand\ without\ air \end{pmatrix} / \left(total\ mass\right) x\ 100 \quad (17)$$

where the total mass refers to the total mass of injected particulate material collected at the sieves. A summary of results is shown in Table 3. As it is apparent the gas curtain is effective as far as particle separation is concerned. The same sort of results also appear for combinations of injection ring and gas curtain. The results presented by Mendonça [10] reinforce the purpose of removing small sized particles using bottom gas injection revealing the positive effect of increasing the gas rate and justifying the position of the dam halfway between the shroud and strands in the tundish model.

When gas is injected through a ring around the left strand the overall pattern changes remarkably at this this side. As it can be seen in Figure 7 the gas curtain directs the flow upwards moving the particles towards the surface. A recirculating flow structure is formed around the gas curtain, region labeled A; before being sucked by the gas curtain the liquid is forced downwards, region labeled B.

A single porous dam located at half distance nozzle – strand affects considerably the overall flow, as can be seen in Figure 8a. Again the main effect is to direct the flow and particles towards the surface, the remaining flow structure adjusting itself to this new feature.

As shown before the best results were achieved by simultaneous injection through the dam and ring. The resulting flow structure is shown in Figure 8b. As before the gas curtains direct the flow upwards. Zhong et al. [11]

Table 3. Percent of inclusions collected at the strand with air injection, E1

Ring		Dam		Ring & Dam	
average	Standard deviation	average	Standard deviation	average	Standard deviation
9.39	2.33	20.79	5.16	2.52	0.46

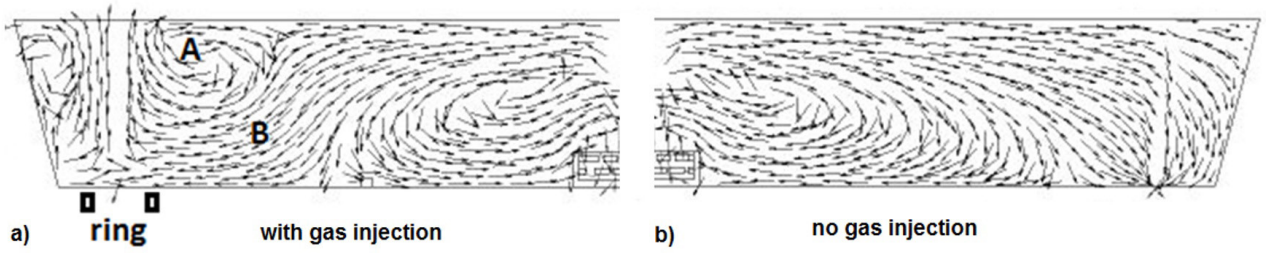

Figure 7. (a) gas purging through a ring around the left side strand at 3 lpm; (b) side with no gas.

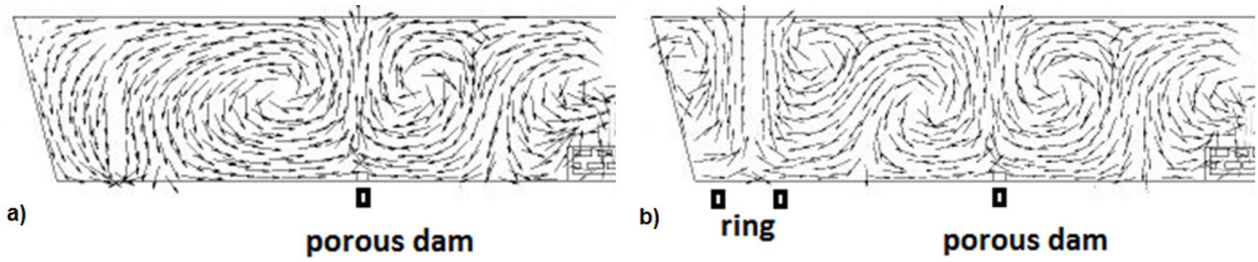

Figure 8. (a) Porous dam purging gas at 3 lpm; (b) combination of porous dam and ring purging at 3 lpm.

varied the position of the porous dam alongside the use of impact pads, weir and a short dam concluding that the gas bubbling increased dramatically the peak concentration time, plug flow volume and decreased the dead volume of the tundish. Generally speaking, the overall flow field is far from the classical view of a combination of perfect mixing region followed by plug flow region and some dead region. There are many circulating flow regions. The role of gas is to act as a barrier hauling liquid and particles towards the surface – slag layer.

4 CONCLUSIONS

Inclusions as small as 30μm are not expected to be significantly removed in a tundish regardless of the proportions of perfect mixing and piston flow regions.

Dead volumes decrease the effective volume available for fluid flow. This could lead to higher interfacial velocities and slag entrainment. Otherwise, steel cleanness will not be affected.

Inclusion collision and coalescence may be effective inside the perfect mixing region. However, the residence time is short and the size distribution of inclusion hauled to the piston flow region should not change in a sizable way.

Gas injection in the tundish can be an effective way of improving steel cleanness as the flow modification that directs the fluid towards the surface leads to a fraction of inclusions collected at the gas assisted strand smaller than 3%.

Acknowledgements

The authors like to thank the support of the Federal University of Ouro Preto and CAPES, CNPq, REDEMAT and Gorceix Foundation for funding this project.

REFERENCES

1 Levenspiel O. Chemical reaction engineering. 3. ed. New York: John Wiley & Sons; 1999

2 Tripathi A, Kumar A, Ajmani SK, Singh JB, Mahashabde VV. Numerical investigation of fluid flow and heat transfer phenomenon inside a single strand tundish of slab caster. Steel Research International. 2015;86:1558-1573.

3 Merder T. The influence of the shape of turbulence inhibitors on the hydrodynamic conditions occurring in a tundish. Archives of Metallurgy and Materials. 2013;58(4):111-117.

4 Cwudzinski A. Numerical, physical, and industrial experiments of liquid steel mixture in one strand slab tundish with flow control devices. Steel Research International. 2014;85(4):623-631.

5 Rogler J. Modeling of inclusion removal in a tundish by gas bubbling [dissertation]. Toronto: Ryerson University; 2004

6 Seshadri V, Silva CA, Silva I, Araújo ES Jr. A physical modelling study of inclusion removal in tundish using inert gas curtain. Tecnologica em Metalurgia, Materiais e Mineração. 2012;9(1):22-29.

7 Saffman PG, Turner JS. On the collision of drops in turbulent clouds. Journal of Fluid Mechanics. 1956;1(1):16-30.

8 Wolf MM. Slab caster tundish configuration and operation: a review. In: Proceedings of 79th Steel Making Conference; 1996 Mar 24-27; Pittsburg, U.S.A. Warrendale: The Iron & Steel Society; 1996. p. 367-381.

9 Sahai Y, Emi A. Criteria for water modeling of melt in continuous casting tundishes flow and inclusion removal. ISIJ International. 1996;39(9):1166-1173.

10 Mendonça AFG. Avaliação do efeito da injeção de gás sobre a flotação de inclusões em um distribuidor de lingotamento contínuo [dissertation]. Belo Horizonte: UFMG; 2016.

11 Zhong LC, Li LY, Wang B, Zhang L, Zhu LX, Zhang QF. Fluid flow behaviour in slab continuous casting tundish with different configurations of gas bubbling curtain. Ironmaking & Steelmaking. 2008;35(6):436-440.

Received: 24 Jan. 2017
Accepted: 14 June 2017